Reaction of I_2 with the (001) surfaces of GaAs, InAs, and InSb. I. Chemical interaction with the substrate

P. R. Varekamp
Department of Physics, Materials Physics, Royal Institute of Technology, S-100 44 Stockholm, Sweden

M. C. Håkansson
Department of Synchrotron Radiation Research, Institute of Physics, Lund University, Sölvegaten 14, S-223 62 Lund, Sweden

J. Kanski
Department of Physics, Chalmers University of Technology, S-412 96 Göteborg, Sweden

D. K. Shuh*
Department of Physics, University of California, Riverside, California 92521
and Materials Sciences Division, Lawrence Berkeley National Laboratory, Berkeley, California 94720

M. Björkqvist and M. Gothelid
Department of Physics, Materials Physics, Royal Institute of Technology, S-100 44 Stockholm, Sweden

W. C. Simpson†
Department of Physics, University of California, Riverside, California 92521
and Materials Sciences Division, Lawrence Berkeley National Laboratory, Berkeley, California 94720

U. O. Karlsson
Department of Physics, Materials Physics, Royal Institute of Technology, S-100 44 Stockholm, Sweden

J. A. Yarmoff
Department of Physics, University of California, Riverside, California 92521
and Materials Sciences Division, Lawrence Berkeley National Laboratory, Berkeley, California 94720

(Received 11 October 1995)

InAs(001)-$c(8\times2)$, InSb(001)-$c(8\times2)$, and several reconstructions of GaAs(001) are exposed at room temperature to iodine molecules (I_2). Low-energy electron diffraction (LEED) and synchrotron soft x-ray photoelectron spectroscopy (SXPS) are employed to study the surfaces as a function of I_2 dose and sample anneal. In the exposure range studied, GaAs and InAs become saturated with I_2, resulting in removal of the clean surface reconstruction and the formation of a very strong 1×1 LEED pattern. Iodine bonds primarily to the dominant elemental species present on the clean surface, whether it is a group-III or -V element. The InSb(001)-$c(8\times2)$ reconstruction is also removed by I_2 adsorption, and a strong 1×1 LEED pattern is formed. SXPS data, in conjunction with scanning tunneling microscopy images, however, reveal that InSb(001)-$c(8\times2)$ does not saturate at room temperature, but is instead etched with a preferential loss of In. Heating the iodine-covered group-III-rich InAs(001)-$c(8\times2)$ and InSb(001)-$c(8\times2)$ surfaces causes removal of the iodine overlayer and transformation to a group-V-rich reconstruction. When the iodine-covered As-rich GaAs(001)-$c(2\times8)$ surface is heated to remove iodine, however, the $c(2\times8)$ reconstruction is simply regenerated. [S0163-1829(96)12427-9]

I. INTRODUCTION

The reactions between halogens and III-V semiconductor surfaces have been the focus of a number of recent fundamental studies due to their important industrial applications.[1] At sufficiently high temperatures and pressures, halogens or halogen-containing compounds can etch III-V semiconductors, which makes these reactions appropriate for use in device processing.[2–5] Below the steady-state etching temperature, however, dosing a III-V semiconductor surface with a halogen in ultrahigh vacuum (UHV) can result in the formation of ordered overlayer structures, which are amenable to exploring questions of basic physics and chemistry.[6–11]

Iodine and bromine have received less attention with respect to their reactions with III-V semiconductor surfaces that have fluorine and chlorine. Interest in the study of iodine, in particular, has increased recently due to the relatively higher volatility of the reaction products formed.[12,13] This aspect is attractive from an industrial standpoint, as it translates directly into lower device processing temperatures.[14–16] This is an especially important feature for the In-containing III-V semiconductors, which have low dissociation temperatures.

Previous fundamental studies of the room temperature (RT) reaction between I_2 and GaAs or InSb have found that etching can often result. For example, mass spectroscopy

measurements showed that Ga and As are removed continuously when an I_2 beam impinges on GaAs($\overline{1}\overline{1}\overline{1}$) at RT, which indicates that steady-state etching is occurring.[17] Also, the nearly continuous uptake of iodine on GaAs(110) suggests that this surface is etched at RT, as well.[18,19] Evidence for the RT etching of InSb(001) is given in the current work from an analysis of scanning tunneling microscopy (STM) images and synchrotron soft x-ray photoelectron spectroscopy (SXPS) data as a function of I_2 exposure. The results further show that the reaction between I_2 and GaAs depends on the crystal face. In contract to the ($\overline{1}\overline{1}\overline{1}$) and (110) surfaces, which are etched at RT, GaAs(001) instead becomes saturated with iodine. Note that our previous report of RT etching of GaAs(001)-4×1 by I_2 was incorrect.[9]

One of the remarkable features of these RT I_2 etching reactions is that the low-energy electron-diffraction (LEED) pattern shows that the near-surface region remains well-ordered while the surface is being etched. For example, dosing either the Ga-rich ($\sqrt{19}\times\sqrt{19}$)R23.45° or As-rich 2×2 reconstructions of GaAs($\overline{1}\overline{1}\overline{1}$) with I_2 at RT induces a 1×1 LEED pattern, even though steady-state etching is believed to occur.[17] A 1×1 LEED pattern is also observed when the In-rich $c(8\times2)$ or Sb-rich $c(4\times4)$ reconstructions of InSb(001) are dosed with I_2,[10,11] but, as will be shown below, I_2 etches InSb(001)-$c(8\times2)$ at RT. The observation of an ordered halogen overlayer during etching at RT is in contrast to the reactions of GaAs with chlorine and fluorine, where the reaction produces disorder in the near-surface region.[20,21] This tendency for I_2 to be a ''gentler'' etchant is important in semiconductor device processing, where a minimal amount of etchant-induced disorder is desired.[14]

After a III-V semiconductor surface has been reacted with I_2, the removal of iodine by annealing generates a clean surface terminated by a group-V element, i.e., I_2 dosing and removal changes a group-III-rich surface to a -V-rich surface, but leaves an initially V-rich surface unchanged. For example, iodine removal is complete after heating either the Ga-rich ($\sqrt{19}\times\sqrt{19}$)R23.45° or As-rich 2×2 reconstructions of GaAs($\overline{1}\overline{1}\overline{1}$) to 600 K, revealing an As-rich 2×2 reconstruction.[17] Likewise, annealing either the iodine-covered In-rich $c(8\times2)$ or the iodine-covered Sb-rich $c(4\times4)$ reconstructions on InSb(001) produces a $c(4\times4)$ clean surface after annealing.[10,11] Exposing a Ga-rich GaAs(001)-4×1 surface to I_2 and then heating the iodine off results in the formation of an As-rich GaAs(001)-$c(2\times8)$ surface.[9] The current results further show that when a GaAs(001)-$c(2\times8)$ surface is dosed with I_2, removal of the iodine by heating simply regenerates the $c(2\times8)$ reconstruction.

This work explores the RT reaction of I_2 with the (001) faces of three III-V semiconductors using core-level SXPS and STM as a function of I_2 exposure and postannealing temperature. The particular substrates, crystal face, and surface reconstructions studied here were chosen for the following reasons. The GaAs, InAs, and InSb substrates are readily available commercially and, in contrast to phosphorous-containing compounds, they consist of elements present in conventional solid-source molecular-beam epitaxy (MBE) systems. The (001) face has particular technological importance and can be prepared with a variety of different surface structures and stoichiometries. A comparison of I_2 reactions with differently prepared surfaces of the same substrate allows conclusions to be made regarding the influence of surface structure and stoichiometry on the surface chemistry. The choice of specific surface structures was based partly on their relative ease of preparation, and partly on the existence of information in the literature about the clean surfaces. For example, although the atomic structures of all (001) surfaces are not completely agreed upon, the $c(8\times2)$, $c(2\times8)$, and $c(4\times4)$ reconstructions present on the (001) crystal face are commonly believed to be superstructures composed of 4×2 unit cells, such as the one shown in Fig. 1.[22–28]

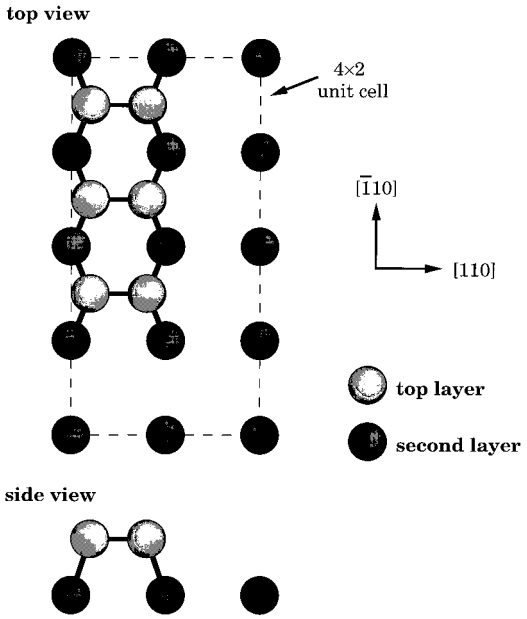

FIG. 1. Atomic-scale schematic diagram of a 4×2 unit cell, composed of two atomic layers of substrate atoms. Through different combinations of these ''building block'' cells, superstructures can be created which form the $c(8\times2)$, $c(2\times8)$, and $c(4\times4)$ reconstructions of clean III-V (001) surfaces (Refs. 22–28).

The format of the presentation is as follows. In Paper I, the interaction between iodine and the individual elements in the III-V semiconductors is ascertained via the intensities and shapes of the substrate core-level spectra. Paper I also contains an STM examination of the large-scale modifications of the InSb surface caused by etching. In Paper II, the structure of the overlayer itself is discussed via SXPS measurements of the I 4d core level and STM.[29] The presentation in Paper I is divided into three sections: (a) the absorption on and saturation of GaAs(001) and InAs(001), (b) the adsorption on and RT etching of InSb(001), and (c) the changes associated with annealing all of the iodine-covered surfaces.

The data presented in part I show that the reaction between I_2 and a III-V semiconductor surface occurs predominantly with the elemental species that is located in the outermost atomic layer. The InAs(001)-$c(8\times2)$ and InSb(001)-$c(8\times2)$ surfaces, which are dominated by group-III-element atoms, show more reaction between iodine and the top In layer than with the less-accessible -V element. The III-V semiconductor surfaces dominated by the -V element, e.g., GaAs(001)-$c(2\times8)$ and GaAs(001)-$c(4\times4)$, display greater reaction with As and little to no interaction with the buried

Ga. This shows that the reaction with I_2 does not disrupt the surface to a great extent. The results also indicate that iodine can form bonds to both group-III and -V elements.

II. EXPERIMENTAL PROCEDURE

Many different surfaces were prepared and exposed to I_2, including the sputtered and annealed group-III-rich $c(8\times2)$ present on all three substrates (also sometimes called 4×1, depending on the quality of the LEED pattern), the sputter-anneal-prepared GaAs(001)-4×6, and the MBE-prepared group-V-rich GaAs(001)-$c(2\times8)$ and -$c(4\times4)$ surfaces. The MBE chamber is attached directly to the beamline and is equipped with reflection high-energy electron diffraction and five effusion cells. The system is capable of growing high-quality material with a characterized background p-type doping of 3.5×10^{14} cm^{-3} (77 K) and GaAs hole mobility of 7500 $cm^2\ V^{-1}\ s^{-1}$ (77 K).

All samples were In glued to 5-mm-thick Mo sample holder blocks, except for InSb(001), which was attached to a Mo sample holder via thin Ta wires. Annealing was performed radiatively from behind the sample holder. Because of the design of the bayonet-style sample transfer system, the K-type thermocouple used for temperature measurement was attached to the cup which held the sample holder. Thus, the temperature measured by the thermocouple is not exactly that of the sample surface. The thermocouple-derived temperatures were calibrated for GaAs(001) with an infrared pyrometer at 515 °C, but there is an estimated uncertainty of ±50 °C at other temperatures.

A UHV-compatible solid-state electrochemical cell, which emits a collimated beam of molecular I_2,was used to dose the surfaces.[30] A solid pellet of pure AgI is the active component of the source. The cell was operated at temperatures between 100 and 200 °C. Exposures were recorded in units of μA min, which represents the operating current of the cell integrated over the dosing time. The current results from ionic flow of I^- through the pellet, and is thus proportional to the amount of I_2 produced. The pressure in the UHV chamber never left the 10^{-10}-mbar scale during dosing. For a given pellet, the amount of I_2 represented by an exposure in μA min is linear in both current and time, as was determined by experiments conducted in an separate chamber containing only an electrochemical cell and a mass spectrometer. For a given III-V (001) surface, the use of different AgI pellets resulted in iodine uptakes within an order of magnitude of each other.

The synchrotron photoelectron spectroscopy was performed at the toroidal-grating monochromator beamline 41 at MAX-lab in Lund, Sweden.[31] All I_2 exposures and SXPS measurements were conducted in the main analysis chamber (pressure $\sim1\times10^{-10}$ mbar). All photoemission measurements were performed at room temperature. The electron spectrometer is a goniometer-mounted hemispherical analyzer (VSW) with an angular resolution of 2°. The total (photon plus electron) energy resolution was better than 0.2 eV. The angle between the surface normal and the p-polarized synchrotron beam was 45°. All spectra were normalized by the photoelectron yield from a gold mesh.

In the cases that were tested, no effects due to electron- or photon-stimulated desorption were observed. This was determined by analyzing core-level shapes and intensities before and after examining the surface with LEED or exposing the surface to zero-order light from the monochromator for 5 min. The stability of InSb(001) surfaces reacted with I_2 at RT with respect to electron- and photon-beam damage has been reported previously.[10,32]

The STM images were collected with a commercial Omicron instrument (base pressure 3×10^{-11} mbar). Sample surfaces were prepared in a connecting chamber (base pressure 1×10^{-10} mbar) equipped with LEED, Auger electron spectroscopy, a mass spectrometer, a sputter gun, and an electron bombardment sample heater. The samples were transferred to the STM chamber entirely under UHV. The STM tips were prepared from W wires by chemical etching. All images in this paper were collected in constant current mode with the sample biased at a negative voltage relative to the STM tip. Thus, the images display only the filled states of the surface. The InSb(001) samples studied with STM were n type, doped with Te to a level of $2.3–3.6\times10^{15}$ cm^{-3}. The wafers were attached to a Ta sample holder plate via Ta foil spot-welded around the edges. The $c(8\times2)$ surface was prepared by several cycles of sputtering with 500-eV Ar^+ ions at an angle of 45° with respect to the surface normal in the [110] azimuth, followed by annealing to 350–400 °C. The off-normal sputtering was found to produce asymmetric terraces for InSb(001), lengthened in the sputtering direction, as previously observed.[22] The samples were used only after an excellent LEED pattern was obtained. The surfaces prepared in this way contained large flat terraces on the order of 500 Å$\times$1000 Å.

III. RESULTS AND DISCUSSION

A. Adsorption of I_2 on GaAs(001) and InAs(001)

This section describes LEED observations from the InAs(001)-$c(8\times2)$, GaAs(001)-4×1, -4×6, -$c(2\times8)$, and -$c(4\times4)$ surfaces as a function of I_2 exposure, as well as SXPS measurements of the In-rich InAs(001)-$c(8\times2)$ surface and the As-rich GaAs(001)-$c(2\times8)$ and GaAs(001)-$c(4\times4)$ surfaces exposed to I_2. It is found that I_2 saturates all of these surfaces in the exposure range investigated.

LEED was performed alone and as part of the SXPS experiments to determine how the long-range surface structure changes with I_2 exposure. After sufficient exposure, all the (001) surfaces formed strong and sharp 1×1 patterns with a relatively weak, but observable, background intensity. This occurred with all three materials and was independent of the initial clean surface reconstruction. It is important to emphasize that the 1×1 spots after I_2 saturation had a significantly higher intensity than in the clean surface pattern. This is consistent with the fact that the large negatively charged iodine atoms are excellent scatterers. The high intensity of the LEED pattern and the lack of higher-order spots from the I_2-saturated surfaces suggest that both the iodine on the surface and the substrate beneath are ordered within a 1×1 unit cell. Thus, the clean surface reconstruction of each of these (001) III-V semiconductor surfaces is removed by reaction with I_2.

The LEED behavior of the GaAs(001)-4×6 surface as a function of I_2 exposure, which is representative of the other surfaces studied, showed a smooth change from the clean

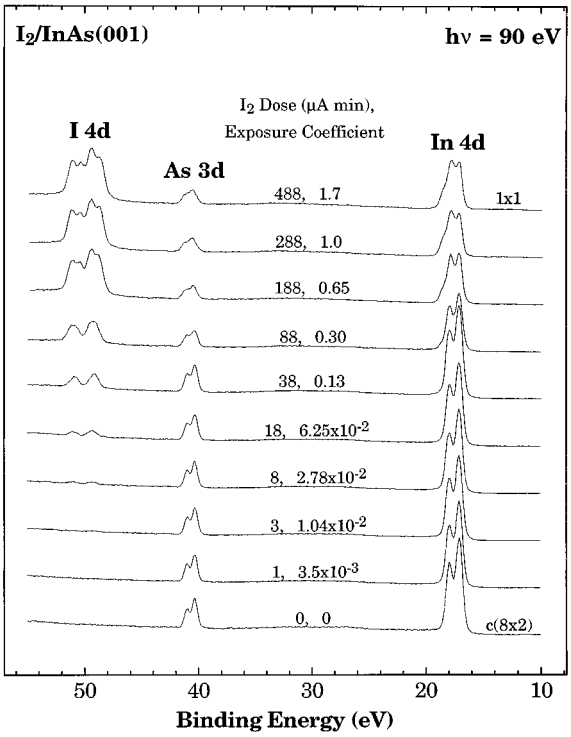

FIG. 2. Photoelectron spectra of the shallow core levels from InAs(001)-$c(8\times2)$, collected as a function of I_2 exposure. Each spectrum is labeled with the electrochemical cell dosage and the corresponding exposure coefficient. The spectra are all plotted on the same scale, but are offset from each other for display purposes. Effects due to band bending were removed by assigning the In $4d_{5/2}$ a binding energy of 17.1 eV relative to the valence-band maximum (Ref. 47).

surface pattern of the 1×1 pattern, without the presence of any intermediate ordered patterns. These particular I_2 exposures were performed in a separate chamber containing only LEED, however, and thus cannot be quantitatively compared to the others in this paper. An exposure of ~5 μA min caused a slight increase in the background intensity, without altering the 4×6 LEED pattern. Doubling the I_2 exposure resulted in a further increase of the background and caused the higher-order spots to fade away. After dosing with ~25 μA min, the 1×1 spots became brighter and stronger as compared to the background, and no higher-order spots were visible. At that point, the intensity of the 1×1 pattern was significantly brighter than the initial 4×6 pattern. Finally, additional exposure to I_2 caused no further changes in the LEED, suggesting that the surface had become saturated by I_2. The photoemission results, presented below, give further evidence of saturation.

Figure 2 displays photoelectron ''survey'' spectra ($h\nu=90$ eV) of the shallow core levels collected from InAs(001)-$c(8\times2)$ as a function of I_2 exposure. Since the photoelectron kinetic energies in these data are located near the relatively flat minimum of the electron escape depth curve,[33] the spectra are extremely surface sensitive and each core level probes approximately the same depth within the sample (~6 Å). The continuous increase in the I $4d$ intensity with exposure shows that iodine gradually accumulates on the surface. For all of the surfaces studied, the I_2 exposure was continued until the core levels exhibited no further changes. For InAs(001)-$c(8\times2)$, this occurred after 288 μA min.

After the largest exposures on all three substrates, the I $4d$ core level is composed of two well-separated components. This is exemplified for InAs(001) in the uppermost spectrum of Fig. 2. The two components manifest themselves as four peaks because of the relatively large spin-orbit splitting (~1.7 eV). Possible origins for the two I $4d$ components are discussed in Paper II.[29]

The SXPS spectra also provide the changes in the position of the Fermi level (E_F) with I_2 exposure. Since the initial pinning positions on the particular surfaces studied are unknown, only the movement of E_F can be determined. For each of the (001) surfaces examined, the kinetic energy of the substrate core-level photoelectrons decreased with iodine coverage, indicating that E_F moves closer to the conduction-band minimum (CBM). This result is in contrast to previous measurements of GaAs(110) exposed to XeF_2, Cl_2, Br_2, and I_2, which reported that E_F moves toward the valence-band maximum (VBM).[18,34–37] In addition, it is found that the total change in E_F for InAs and InSb is comparable to, or greater than, the band gaps (0.36 and 0.18 eV, respectively, at RT). This suggests that E_F is pinned above the CBM on the iodine-covered surfaces, which would produce a surface charge accumulation layer. Such an effect has been observed previously on clean InAs surfaces,[38] and on InAs(110) after reaction with O_2 or Cl_2.[39] That E_F is pinned above the CBM of I_2-saturated InAs(001)-$c(8\times2)$ was verified by the observation of conduction-band photoelectrons in normal emission.

In order to quantify the amount of iodine on the surface as a function of exposure, each core level was integrated after subtraction of a linear background. The results are presented in Fig. 3, where each panel contains a plot of the ratio of the total I $4d$ area to the area of each substrate core level as a function of I_2 dose on a log scale. Note that area ratios determined from the high-resolution core-level spectra were always in excellent agreement with those determined from the survey spectra, even though they were collected with different photon energies. This indicates that diffraction and probing depth effects, which depend on the photon energy, only minimally affect the core-level ratios. Note that the error bars in Fig. 3 represent the uncertainty in the determination of the core-level area. This uncertainty, which was always less than 5%, arises primarily from the choice of background.

The data in Fig. 3 show the iodine coverage as a function of exposure. Figures 3(a)–3(c) confirm that there is a smooth uptake of iodine on each surface, and that the surfaces saturate. The nearly exact overlap of the two curves at every point shows that the ratios of the I $4d$ core level to each of the substrate core levels are equal. This behavior is consistent with iodine simply covering the substrate, without the removal of any material. The results for InSb(001) are shown in Fig. 3(d). It is seen that the behavior after the highest I_2 doses is different from the other three surfaces, as will be discussed in detail in Sec. III B below. The saturation of I_2 on GaAs(001) is in contrast to the previously reported behavior of the (110) and $(\bar{1}11)$ faces,[17,18] indicating a crystal face dependence in the reaction of I_2 with GaAs.

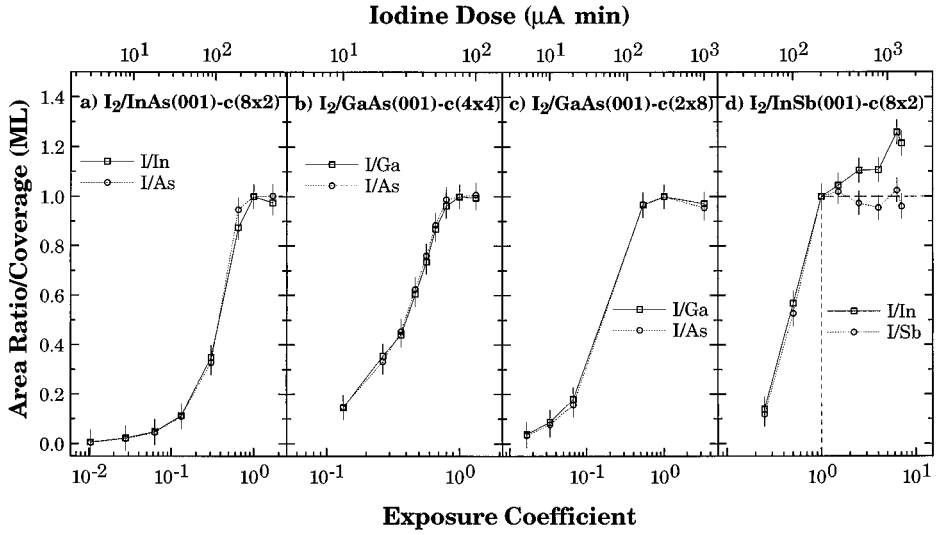

FIG. 3. (a)–(d) Ratios of the core-level areas above the background, shown as a function of the I_2 exposure on a log scale. The iodine–III-element (open squares and solid line) and iodine–V-element (open circles and dashed line) ratios are displayed for each surface. The electrochemical cell dosage for each system is given on the top x axis, while the bottom x axis is the exposure coefficient, as defined in the text. The y axis gives the surface iodine coverage in ML, under the assumption that the saturation coverage is ~1 ML. Uncertainties in the values are indicated by vertical lines around each data point.

The data of Figs. 3(a)–3(c) show similar saturationlike behavior for all three surfaces, but the surfaces do not saturate at exactly the same I_2 dose. Whether this is because of different adsorption chemistry or because of differences in electrochemical cell calibration cannot be determined. Therefore, in order to compare the different surfaces to each other, an exposure coefficient e is defined from the core-level ratio data, such that $e=1$ when the ratios first display saturationlike behavior. The ratios in Fig. 3 are then normalized to 1.0 at $e=1$. Note that each panel in Fig. 3 has a top x axis, which displays the I_2 dose from the electrochemical cell, and a bottom x axis showing the exposure coefficient.

The amount of iodine present on the surfaces at saturation is most likely 1.0 ML. This conclusion is drawn from the presence of a 1×1 LEED pattern at saturation, together with the fact that multilayers of iodine on the surface at RT are not expected to occur. Additional support for a saturation coverage of 1.0 ML comes from STM data of iodine-covered InSb(001) presented in Paper II,[29] which show approximately one adsorbate atom per unit cell. Thus, the area ratios of Fig. 3 are numerically equal to the iodine coverage in ML, and this figure thereby provides a calibration between exposure and coverage.

Note, however, that it is not sufficient to just specify a coverage in order to uniquely describe a particular surface structure and composition. This is why the exposure coefficient, rather than the coverage, is used as a label in the remainder of this paper. For example, as shown in Sec. III B below, exposures in excess of $e=1$ for InSb act to remove In, while they do not change the iodine coverage. Thus, two surfaces with the same iodine coverage can have very different compositions. Also, as shown in the annealing studies of Sec. III C below, substrate material can be removed inhomogeneously when an iodine-covered surface is heated. Thus, two surfaces with equivalent coverages can have remarkably different stoichiometries if one is produced by iodine dosing and the other by overdosing and annealing. These considerations justify the use of exposure coefficients to uniquely specify a particular dosed surface, and the use of temperatures to describe annealed surfaces.

High-resolution spectra were collected as a function of I_2 exposure in order to more closely study the changes occurring in the substrate core levels. Representative spectra are shown in Fig. 4 for InAs(001). Four spectra are displayed for each substrate core level, i.e., one collected from the clean $c(8\times2)$ surface and three from surfaces exposed to I_2. The most obvious changes to both core levels occurs on the high-binding-energy (BE) sides. This is expected for reaction with a very electronegative element, such as iodine, which draws charge away from the atom to which it is bound. From the raw data, it is clear that the In $4d$ core level changes more than the As $3d$ level, indicating that iodine reacts more with In atoms than with As. The most likely reason for this is that there are more In atoms available at the surface for reaction, since the $c(8\times2)$ reconstruction is In-rich.

In order to determine the chemical environments of the substrate atoms after I_2 reaction, the high-resolution core-level spectra were numerically fit to a sum of Gaussian-broadened Lorentzian spin-orbit split doublets. Before fitting a spectrum, a cubic spline fit to the background on both sides of the core level was subtracted from the raw data. The resultant spectrum was then fit with the fewest number of doublets possible, each possessing the parameters given in Table I. The fit parameters were initially selected from the literature.[24,40–42] but were then optimized for the present data.

The fitting procedure is not deterministic in that it does not yield a unique solution. Thus, in order to obtain the most physically reasonable solution, many constraints were imposed. In the final evaluation, a fit to a particular core level was only deemed acceptable if it fit into the set of data as a whole, with no sudden changes in the number of components or fit parameters as small changes were made to the surface.

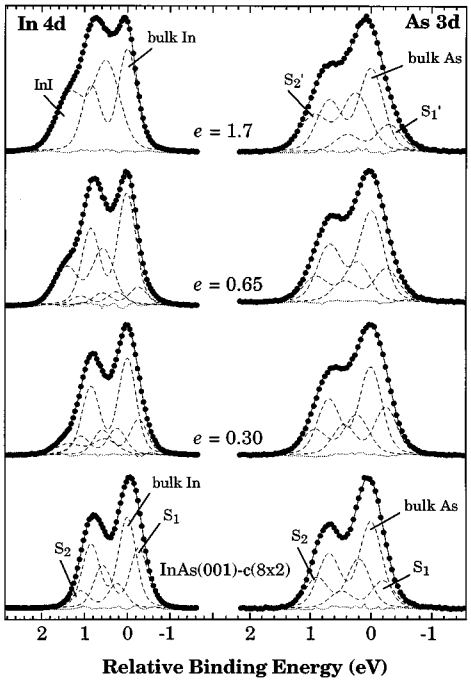

FIG. 4. High-resolution core-level spectra collected in normal emission from the InAs(001)-$c(8\times2)$ surface dosed with an amount of I_2 given by the exposure coefficient e. Each spectrum has been numerically fit to a number of Gaussian-broadened Lorentzian doublets using the fit parameters in Table I. The raw data are given by filled circles, the individual fit components by dashed lines, the total fit result by a solid line, and the fit residuals by a dotted line. The binding energy scale is presented relative to the substrate $d_{5/2}$ component. The In $4d$ core levels in panel (a) were collected with a photon energy of 82 eV, except for the clean $c(8\times2)$ surface where the photon energy was 79 eV. The As $3d$ core levels in panel (b) were collected with a photon energy of 102 eV.

One of the assumptions in the fitting procedure is that for a given element, the spin-orbit splitting is always fixed at the same value. Another is that for a given chemical system, for example, all I_2 doses on InAs(001), the Lorentzian width (LW) for each element has a fixed value. Different choices for the method of background subtraction were, however, found to influence the LW determined from the fits by up to ±0.1 eV. Additional constraints were placed on the energy separations between components and the Gaussian width (GW) of each component, so that they remained constant over as wide a range of coverages as possible for a given chemical system. Finally, the branching ratios for each doublet were constrained to be the same within a particular spectrum. Typical error values in a fit parameter, i.e., the amount a parameter can change while still producing an acceptable fit, were approximately ±0.02 eV for the separations between components and $\sim10\%$ for the component intensities.

As a further aid to finding appropriate numerical fits, spectra collected in normal emission were compared to spectra collected from at least one other angle, usually 60° from the surface normal. Although only normal emission spectra are shown, off-normal emission spectra were recorded from nearly all of these surfaces. A fit was judged to be acceptable if both normal and off-normal spectra could be fit with the same number of components at the same positions. This method proved to be one of the most stringent constraints of all. If any energy shifts occurred as a function of angle, only those on the order of one channel in the raw data (27 meV) or less were permitted. The only parameters that were allowed to vary as a function of emission angle were the peak intensities, the GW's, and the branching ratios. The branching ratio variations were always less than 15%.

The relative BE's determined for the shifted components, relative to the bulk component, are given in Table II for all of the surfaces studied. The table is divided into sections, representing (1) the initial clean surface, (2) the I_2-dosed surface, (3) the surface following light annealing, and (4) after complete removal of the iodine by annealing. Shifted components found on the clean surface are designated by ''S'' and a subscript. After a surface was dosed with I_2, the component notation is modified with a ''prime,'' indicating that there could be an additional, unresolved contribution to the component. One reason to suspect this possibility is the observation of small movements in the BE's with I_2 exposure, as seen in Table II. New components which appear for a given core level are labeled by ''mono-'' or ''di-'' in the table, to indicate that the new component is attributed to a monoiodide or di-iodide of the given element.

The results of the fitting procedure for InAs(001)-$c(8\times2)$, shown in Fig. 4, indicate that a new component, attributed to indium monoiodide (InI), appears on the high-BE side of the In $4d$ level with I_2 exposure. When the surface becomes saturated, all of the In clean surface components have disappeared, and only contributions from substrate In and InI are observed. The As $3d$ also shows an increase on the high-BE side, which is due to the growth of the component labeled S_2'. Note, however, that the persistence of S_1' at lower BE suggests that unreacted second-layer As atoms may also con-

TABLE I. Table of the parameters employed in the fits to the high-resolution core-level spectra. Given for each core level are the photon energy used in collection, the spin-orbit splitting (SO), the branching ratio (BR), and the Lorentzian full-width at half-maximum (LW). Changes in the values of the BR's as a function of dose or anneal are noted in the table, with an arrow illustrating monotonic movement and a dash representing a range.

Substrate	InAs(001)-$c(8\times2)$		InSb(001)-$c(8\times2)$		GaAs(001)-$c(4\times4)$		GaAs(001)-$c(2\times8)$	
Core-level	In $4d$	As $3d$	In $4d$	Sb $4d$	Ga $3d$	As $3d$	Ga $3d$	As $3d$
$h\nu$ (eV)	79,82	102	82,96	96	60	81	80	102
SO (eV)	0.85	0.69	0.85	1.25	0.45	0.69	0.45	0.69
BR	1.43→1.58	1.60–1.65	1.39→1.55	1.36→1.41	1.6–1.85	1.50–1.75	1.62	1.50
LW (eV)	0.13	0.10	0.13	0.14–0.15	0.16	0.17	0.17	0.10

TABLE II. The binding energies (BE's), relative to the bulk component, for the shifted core-level components. The data are divided into sections representing (1) the initial clean surfaces, (2) the I_2-dosed surfaces, (3) the heated iodine-covered surfaces, and (4) the surfaces after iodine removal. ''Mono-'' and ''di-'' indicate new components attributed to iodine bonding. For the identities of the different ''*S*'' components, see the appropriate figures of the high-resolution spectra. Changes in the values of the relative BE's as a function of dose or anneal are noted in the table, with an arrow illustrating monotonic movement and a dash representing a range.

Substrate	InAs(001)-$c(8\times2)$		InSb(001)-$c(8\times2)$		GaAs(001)-$c(4\times4)$		GaAs(001)-$c(2\times8)$	
Core-level	In 4*d*	As 3*d*	In 4*d*	Sb 4*d*	Ga 3*d*	As 3*d*	Ga 3*d*	As 3*d*
(1) Clean:								
S_1 (eV)	−0.27	−0.20	−0.28	−0.31	0.33	−0.40	0.35	−0.46
S_2 (eV)	0.24	0.20	0.29	0.31		0.40		0.46
(2) Dosing:								
S_1' (eV)	−0.27	−0.20→−0.3	−0.28	−0.31→−0.3	0.33→0.40	−0.40→−0.5	0.35	−0.46
S_2' (eV)	0.24	0.20→0.25	0.29	0.31→0.35		0.40→0.50		0.46
mono (eV)	0.52→0.50		0.54→0.38					
di (eV)				0.70		0.90		1.0
(3) Heating:								
S_1'' (eV)	0.35	−0.3→−0.24		−0.30				
S_2'' (eV)		0.25→0.22	0.38	0.35				
mono (eV)	0.50→0.48							
(4) Clean:	InAs(001)-$c(2\times8)$		InSb(001)-$c(4\times4)$					
S_1''' (eV)	0.35	−0.24		−0.30				
S_2''' (eV)		0.22		0.35				

tribute to the high-BE side of the As 3*d*. Thus, it is not clear whether the increase in S_2' represents the formation of arsenic monoiodide (AsI), changes in the second-layer As signal, or some combination of the two.

High-resolution substrate core-level spectra were also collected from the GaAs(001)-$c(2\times2)$ and -$c(4\times4)$ surfaces after various I_2 exposures. Figures 5 and 6 show the spectra collected from the clean and saturated surfaces. Again, it is clear from the raw data that the outermost substrate element is the one most affected, which, for both of these reconstructions, is As. In both As 3*d* spectra collected from saturated surfaces, the S_2' component is attributed primarily to AsI, although a contribution from unreacted elemental As cannot be completely ruled out. The increase in the GW of the S_1' component in the Ga 3*d* spectrum of the $c(2\times8)$ surface most likely indicates the formation of a small amount of gallium monoiodide (GaI). The Ga 3*d* on the $c(4\times4)$ surface, on the other hand, did not change at all after I_2 adsorption. This behavior is also consistent with reaction only at the outermost atomic sites, since the $c(4\times4)$ surface is thought to have no exposed Ga.[26,41,43]

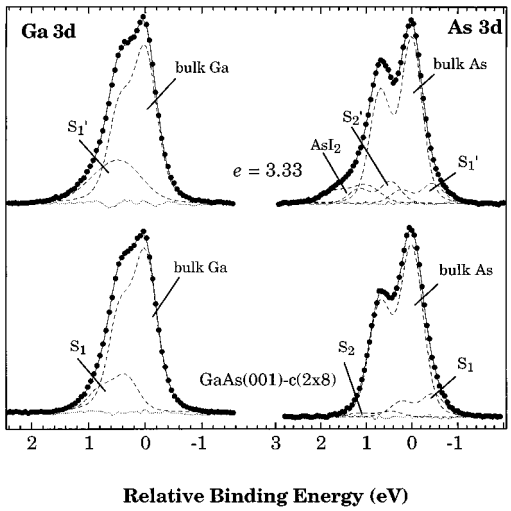

FIG. 5. High-resolution core-level spectra collected in normal emission from clean and I_2-saturated GaAs(001)-$c(2\times8)$, together with the results of a numerical fitting procedure. The legend for the symbols is the same as that in Fig. 4.

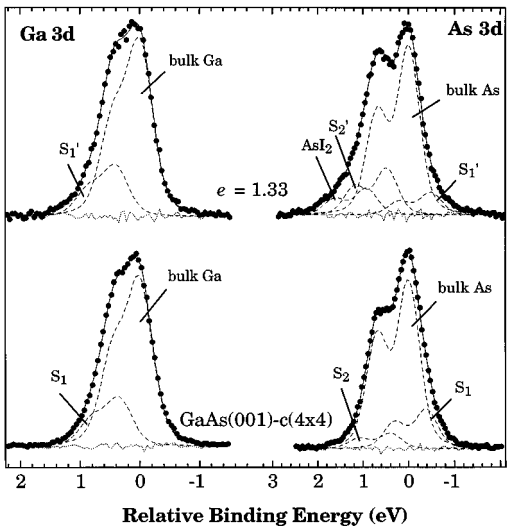

FIG. 6. High-resolution core-level spectra collected in normal emission from clean and I_2-saturated GaAs(001)-$c(4\times4)$, together with the results of a numerical fitting procedure. The legend for the symbols is the same as that in Fig. 4.

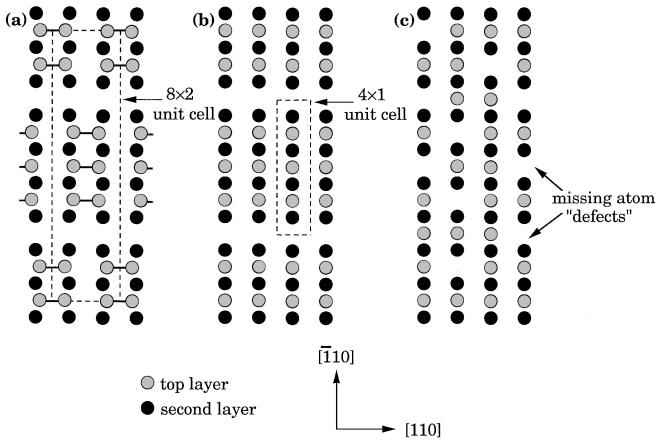

FIG. 7. Atomic-scale diagrams of the changes that can occur when the $c(2\times8)$- or $c(8\times2)$-reconstructed clean surface pictured in (a) is reacted with I_2. If the surface dimers are broken and iodine is attached at each site, the 1×4 or 4×1 symmetry shown in (b) is generated. Allowing the surface atoms to randomly diffuse laterally can generate the structure in (c), which has 1×1 symmetry.

Based on the data presented above, the RT reaction of I_2 with GaAs(001)-$c(2\times8)$, GaAs(001)-$c(4\times4)$, and InAs(001)-$c(8\times2)$ is explained as follows. The adsorption of I_2 results in the breakage of surface dimers and the bonding of iodine to all available sites, at which point the reaction stops and the surface is saturated. The breakage of a majority of the dimer bonds is a necessary condition to remove the twofold symmetry and produce a 1×1 LEED pattern. However, simply breaking the dimers and attaching iodine at each (former) dimer atom site is not sufficient, since there would be ordered rows of missing top-layer atoms that would still produce higher-order LEED spots, or streaks. This is illustrated in the atomic-scale schematic diagrams of Fig. 7, where a clean surface with a $c(8\times2)$ reconstruction in (a) becomes a 4×1 reconstruction after iodine adsorption and dimer bond breaking, as shown in (b). In order to produce an arrangement with a 1×1 LEED pattern, some first-layer atoms must diffuse laterally to produce a random distribution of missing atoms, as shown in Fig. 7(a). These missing atom sites can be viewed as ''defects'' on the surface, and they would be stable as the second-layer atoms are bonded in tricoordinate configurations. Even if the missing atoms were to amount to as much as 0.25 ML, the strong electron scattering of 0.75 ML of ordered iodine atoms would still produce a bright 1×1 LEED pattern. Note that the missing atom ''defects'' may provide additional sites for iodine adsorption. The presence of a secondary adsorption site on InSb(001) has been suggested previously by Mowbray, Jones, and McConville.[32] The present data, however, suggest that only the outermost substrate atoms are bound to iodine. Alternatively, it is possible that some atoms diffuse up from the bulk, or laterally from step edges, and fill in the missing atom defects, which then become sites at which additional well-ordered monoiodides could form.

Since the iodine adsorption reaction results in no extensive disruption of the substrate, it seems logical that a high-quality clean surface would be necessary in order to form a well-ordered 1×1 LEED pattern at saturation. In fact, it was observed that if the initial sputtered and annealed clean surface possessed a fuzzy or high-background LEED pattern, a weak and fuzzy 1×1 pattern resulted after I_2 exposure. In contrast, a beautiful 1×1 LEED pattern was always observed from the high-quality GaAs(001) MBE-prepared surfaces after saturation with I_2.

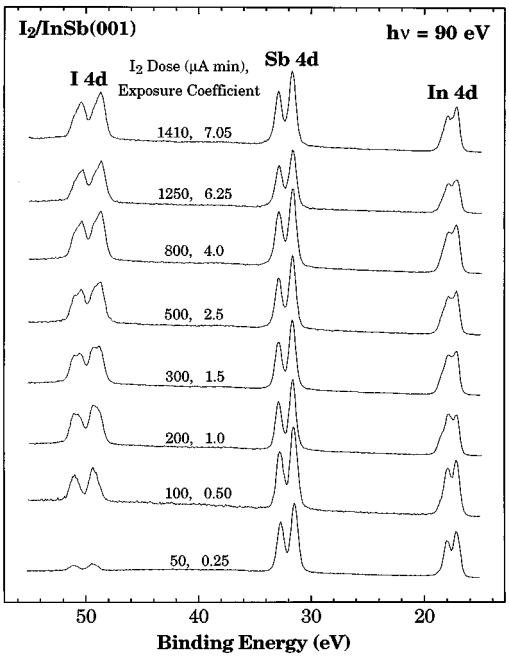

FIG. 8. Photoelectron spectra of the shallow core levels of InSb(001)-$c(8\times2)$, collected as a function of I_2 exposure. Each spectrum is labeled with the electrochemical cell dosage and the corresponding exposure coefficient. The spectra are all plotted on the same scale, but are offset from each other for display purposes. Effects due to band bending were removed by assigning the In $4d_{5/2}$ a binding energy of 17.2 eV relative to the valence-band maximum (Ref. 48).

B. Reaction of I_2 with InSb(001)

This section describes LEED, SXPS, and STM measurements conducted on the In-rich InSb(001)-$c(8\times2)$ surface as a function of I_2 exposure. Iodine is found to etch this surface at RT in the exposure range investigated.

The initial adsorption of I_2 on InSb(001)-$c(8\times2)$ is very similar to that on InAs(001) and GaAs(001). First, the change in LEED from a $c(8\times2)$ pattern to a very strong 1×1, with a noticeable background, shows that the clean InSb(001) surface reconstruction is removed after I_2 adsorption, in agreement with previous work.[10,11] Second, the survey spectra presented in Fig. 8 reveal that the total amount of iodine on the surface saturates, as seen for the other substrates. This occurs after a dose of 200 μA min, and serves to define $e=1$. Third, the high-resolution substrate core-level spectra shown in Fig. 9 show that iodine bonds primarily to the outermost surface element, forming InI. Unlike the GaAs(001) and InAs(001) surfaces, however, Fig. 8 shows that I_2 exposure above $e=1$ on InSb(001) results in further changes to the shape of the I $4d$ level, while its total area remains constant. Shape changes are also apparent in the substrate core levels for $e>1$, particularly for In $4d$, as seen in Fig. 9.

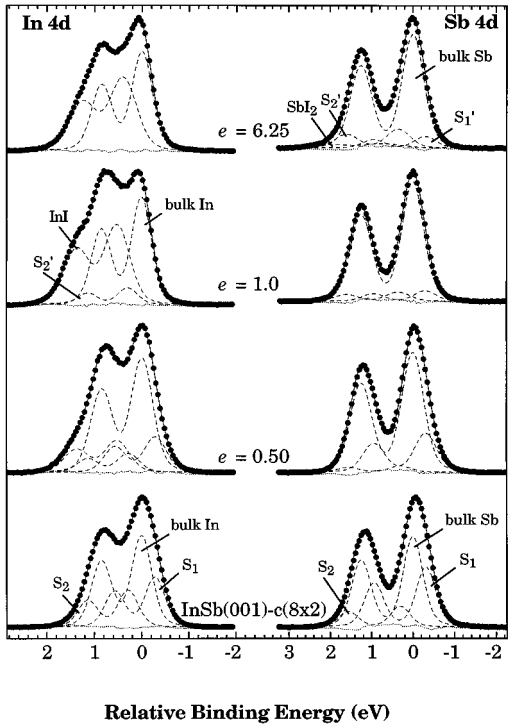

FIG. 9. High-resolution core-level spectra collected in normal emission from clean and I_2-dosed InSb(001)-$c(8\times2)$, together with the results of a numerical fitting procedure. The legend for the symbols is the same as that in Fig. 4. The In 4d core levels in panel (a) were collected with a photon energy of 82 eV, and the Sb 4d core levels in panel (b) were collected with a photon energy of 96 eV.

In order to explore the changes that occur on the InSb(001) surface after it has been completely covered with I_2, i.e., for $e>1$, reacted surfaces were examined with STM. Figure 10 shows two large-scale 1000 Å$\times$1000 Å STM images collected with nearly identical tunneling conditions from I_2-reacted InSb(001)-$c(8\times2)$. The image in (a) was collected after dosing the surface with enough I_2 so that no unreacted areas could be found ($e\sim1$). The image in Fig. 10(b) was collected after dosing the surface in (a) with approximately 50% more I_2 ($e\sim1.5$).

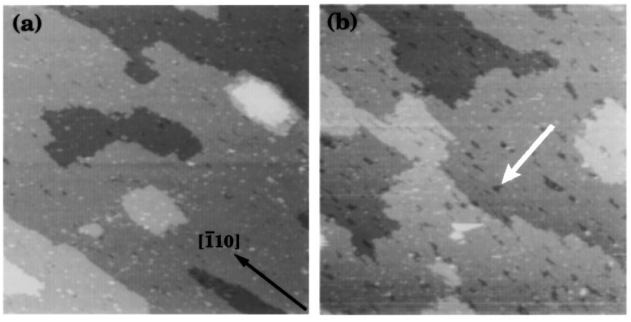

FIG. 10. Two 1000-Å$\times$1000-Å filled state scanning tunneling microscopy images of an InSb(001)-$c(8\times2)$ surface dosed with I_2. The tunneling current is equal to 0.04 nA in each image with the sample biased -2.3 V relative to the tip in (a) and -2.1 eV in (b). The surface in (a) was just completely covered with iodine, while the surface in (b) was dosed with 50% more iodine than in (a). The white arrow in (b) points to an etch pit.

A careful comparison of the two STM images in Fig. 10 shows that I_2 continues to react substantially even after the surface is fully covered. Both images are similar in that they contain large flat terrace regions, with the height difference between any two adjacent terraces corresponding to the double-layer step height of 3.2 Å. The images differ, however, with regard to the profile of the step edges and the number and size of small dark regions on the terraces. For example, the image in (a) contains quite smooth step profiles and squarelike terrace shapes, similar to what is observed in images collected from the clean surface (not shown), and in images available in the literature.[23,25] In panel (b), however, the step edges are much more jagged, so that the terrace shapes are, in general, less symmetric. A white arrow in (b) points to one of the small dark regions present in the image. The dark regions in (a) have an average size of $\sim$100 Å^2 and a density of 1.4×10^{12} cm^{-2}, while those in (b) have an average size and density of $\sim$600 Å^2 and 2.3×10^{12} cm^{-2}, respectively. Thus, there is an increase in the number density and size of the dark regions with exposures. Line scans across these regions confirm that they are deeper than the surrounding areas on the surface. No features were ever imaged within the pits, however, and the depth measurements are thus somewhat uncertain. The measured depths of the pits in both images were quite variable, ranging from 0.5 to 1.5 times the In-Sb double-layer height.

The changes observed in going from Figs. 10(a) to 10(b) are attributed to RT etching of InSb(001). The dark regions are interpreted as etch pits, which result after substrate material is converted into volatile iodide molecules. The transition of the step-edge profile from smooth to jagged is attributed to uneven etching of the step edge. Another observation that can be made from the images in Fig. 10 is that the etch pits are longer in the [110] direction than the [1$\bar{1}$0] direction. This suggests that RT etching occurs more rapidly in the [110] azimuth. Note that inhomogeneous etching cannot be completely decoupled from the possible presence of preferential subsurface damage effects in this azimuth, however, as [110] was also the sputtering direction. Previous STM studies of the etching of GaAs(110) with Cl_2 and Br_2 also reported the formation of etch pits and irregular step edges, which supports the conclusion that I_2 etching of InSb is occurring here.[3,8]

In order to examine changes in the stoichiometry of the near-surface region during the RT etching of InSb(001), the ratio of the In 4d core-level intensity to the Sb 4d intensity is shown in Fig. 11. Different symbols are used to illustrate ratios collected with different photon energies or along different emission angles. For I_2 exposures above $e=1$, i.e., when the area of the I 4d is constant with exposure, the In/Sb ratio decreases with exposure. The small variations from the best-fit line drawn in the figure are most likely due to contributions from diffraction and/or escape depth effects.

Although the decreasing In/Sb ratio as a function of I_2 dose can be due to either a loss of In or an enrichment of Sb in the near-surface region, the indications of etching in the STM data and the presence of primarily indium iodine compounds on the surface suggest that it is most likely due to a preferential removal of In. This conclusion is consistent with

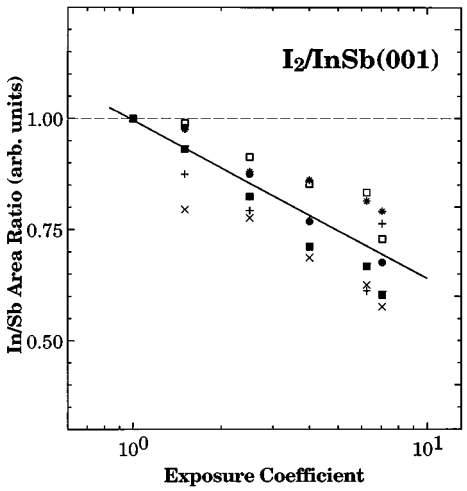

FIG. 11. Ratios of the total area of the In 4*d* to the Sb 4*d* area, from core levels in survey (Fig. 8) and high-resolution (Fig. 9) spectra. All ratios are normalized to 1 at $e=1$. The symbols represent In/Sb collected with photon energies and emission angles of 90 eV/90 eV, 0° (*); 82 eV/72 eV, 0° (+); 96 eV/72 eV, 0° (×); 96 eV/96 eV, 0° (□); 96 eV/96 eV, 60° (■); 82 eV/96 eV, 60° (●). The solid line is a best fit to the data.

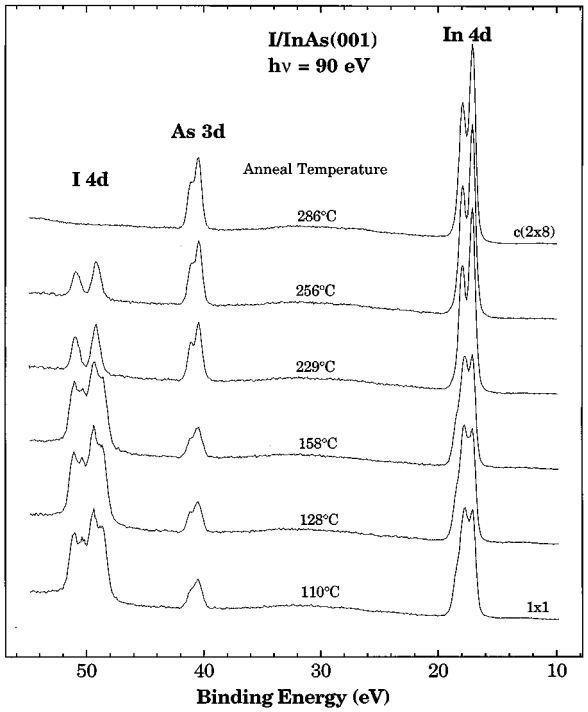

FIG. 12. Photoelectron spectra of the shallow core levels from InAs(001), collected as a function of annealing temperature. Each spectrum is labeled with the approximate annealing temperature (±50 °C). The spectra are all plotted on the same scale, but are offset from each other for display purposes.

the changes in the iodine to substrate core-level ratios shown in Fig. 3(d). These ratios, which do not overlap for $e>1$, indicate that the substrate is not simply being covered by iodine. Since the emission from the I4*d* core level is constant for $e>1$, the amount of iodine on the surface should be constant. Preferential etching of In from the surface would cause the I/In ratio to increase with exposure, which is exactly what is observed in Fig. 3(d). Loss of In would also result in an enrichment of the surface Sb, which would be observed as a decrease in the I/Sb ratio. This is again in agreement with the small decrease observed in Fig. 3(d).

Previous studies have proposed that the iodine overlayer on InSb(001)-$c(8\times2)$ is composed of a full monolayer of iodine atoms bound to a full monolayer of coplanar substrate atoms below.[10,11] Specifically, the coplanar substrate layer is thought to be made up of the 0.75 ML of In which was present in the top layer of the $c(8\times2)$ reconstruction, plus 0.25 ML of Sb which is pulled upwards as a result of the reaction. The main support for this model appears to be a 21% decrease in the In/Sb Auger ratio following I_2 exposure reported by Jones, Singh, and McConville.[11] However, the preferential etching of In at RT, as suggested by the current data, is a more likely explanation for the decrease in the In/Sb ratio. Thus, no evidence is found here for the movement of Sb atoms perpendicular to the surface at RT.

C. Annealing the iodine-covered III-V (001) surfaces

Annealing the iodine-covered (001) surfaces to remove iodine resulted in the change of the LEED pattern from 1×1 to a pattern with higher-order spots indicative of a clean surface reconstruction rich in the group-V element. This was true for all of the surfaces studied, independent of the reconstruction prior to I_2 exposure. Thus, the Ga-rich GaAs(001)-4×1, -4×6, and As-rich GaAs(001)-$c(2\times8)$ surfaces all displayed a $c(2\times8)$ pattern after I_2 saturation and heating. Furthermore, the In-rich InAs(001)-$c(8\times2)$ and InSb(001)-$c(8\times2)$ surfaces were transformed into the V-element-rich InAs (001)-$c(2\times8)$ and InSb(001)-$c(4\times4)$ surfaces by I_2 exposure and removal. These LEED observations show that an I_2 dose and anneal cycle on a (001) III-V semiconductor surface results in the preferential removal of the group-III-element surface species, as has been previously reported[9–11,17] and discussed above in the Introduction.

Figure 12 displays photoelectron survey spectra collected from I_2-saturated InAs(001)-$c(8\times2)$ following annealing to various temperatures. From these spectra, it is apparent that the I_2-saturated surface is quite stable when heated up to ~160 °C. Higher annealing temperatures, however, result in a significant loss of iodine and cause noticeable changes in the substrate core levels. After heating to ~290 °C, all the iodine is removed and the $c(2\times8)$ LEED pattern forms.

An intensity analysis of the core-level areas gives more quantitative information concerning the behavior of the iodine-covered InAs(001) and InSb(001) surfaces with annealing. The upper panels of Fig. 13 show the ratios of the iodine core-level area to each substrate core-level area, determined from survey spectra, such as those of Fig. 12. These ratios also roughly indicate the iodine coverage in ML. The removal of iodine from the surface by annealing is clearly illustrated by these data, which are nearly the reverse of the adsorption data of Fig. 3. The lower panels of Fig. 13 depict the group-III to -V core-level area ratios as a function of annealing temperature. The drop in the ratio of group-III to -V atoms in the near-surface region by a full factor of 2 for both InAs and InSb shows that substantial changes in the surface stoichiometry have occurred. The behavior for

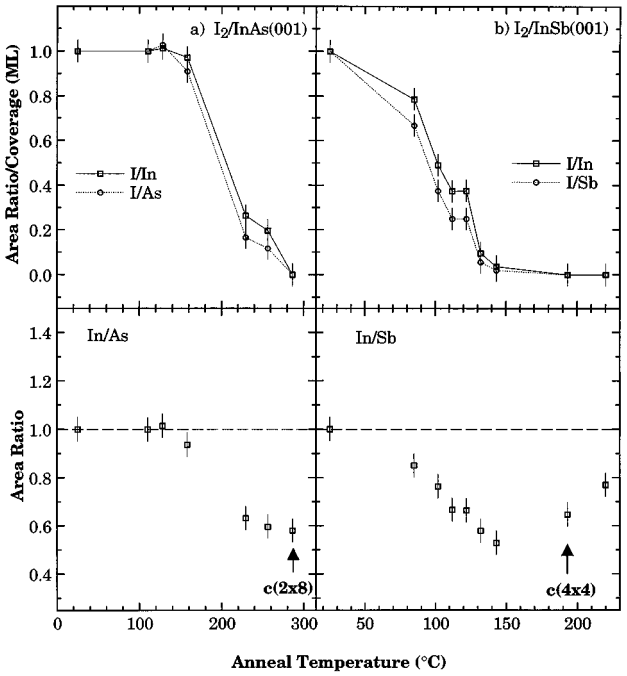

FIG. 13. (a) and (b) Ratios of the survey core-level areas as a function of the annealing temperature. The upper panels display the iodine–III-element (open squares and solid line) and iodine–V-element (open circles and dashed line) ratios, while the bottom panels show the III-element to V-element ratio. The y axis for the upper panels also gives the iodine coverage in ML, under the assumption that the saturation coverage is ~1 ML.

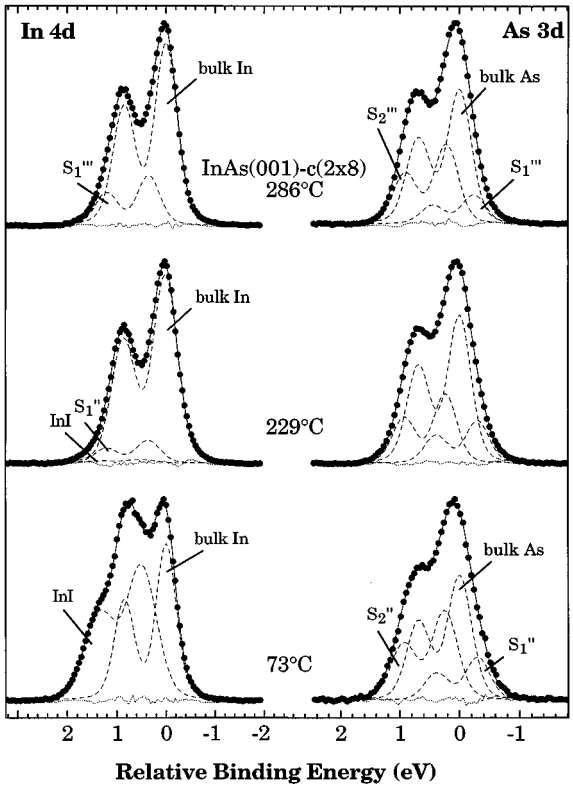

FIG. 14. High-resolution core-level spectra collected in normal emission from I_2-saturated InAs(001) surfaces annealed to the temperature shown, together with the results of a numerical fitting procedure. The legend for the symbols is the same as that in Fig. 4. The photon energies employed are 82 eV and 102 eV for In and As, respectively.

InSb(001)-$c(8\times2)$ observed in Fig. 13(b) agrees with previous Auger spectroscopy measurements by Mowbray and Jones.[10]

The decrease in the III/V ratio by a factor of 2 is attributed to a preferential loss of surface In, just as was observed in Fig. 11 during the RT etching of InSb(001). This conclusion is supported by the high-resolution spectra collected from the iodine-covered surfaces, which show InI to be the dominant surface species prior to annealing, and by the LEED pattern, which is indicative of an Sb-terminated surface after iodine removal. Further support comes from the observation of InI as the predominant desorbing species in preliminary thermal desorption mass spectrometry results for iodine-covered InSb(001).[44]

Additional evidence in support of the removal of In from the surface during heating is found in the high-resolution core-level data. These spectra are shown in Figs. 14 and 15 for the iodine-covered In-rich InAs(001)-$c(8\times2)$ and InSb(001)-$c(8\times2)$ surfaces, respectively. The group-III-element high-resolution core level changes significantly more than the -V-element core level when the surface is heated, just as occurred during dosing. The primary behavior of the In $4d$ core levels collected from these two surfaces is the reduction of the InI component intensity. In the InAs case, the presence of a new surface-related component is observed after high anneal temperatures, whereas no new components are observed for InSb. The lack of resolvable surface components in the In $4d$ level for InSb(001)-$c(4\times4)$ is in agreement with fits published in the literature.[24] For both surfaces, the group-V-element core level changes very little, as is easily seen in the raw data. The changes in the substrate core levels for these two surfaces show that the primary result of annealing an iodine-covered surface is the removal of InI, supporting the conclusions made above.

Note that after annealing the iodine-covered InSb(001) sample to only ~125 °C, the LEED pattern was still a bright and fairly sharp 1×1 with a low background. This shows that even though some etching has occurred, the surface is still very well ordered. A likely explanation for the presence of order is that InI is removed from the surface inhomogeneously, and that the bonding sites of the remaining iodine are not significantly affected by heating to this temperature. The inhomogeneous removal of thin films from semiconductor surfaces during annealing has been reported previously for GaF_3 on GaAs (Ref. 21) and SiO_2 on Si.[45]

It has been previously suggested that an I_2 dose-anneal cycle is an excellent chemical means for producing a group-V-terminated surface on InSb(001) without the use of MBE.[11] Care must be taken, however, if this statement is to be extended to the other III-V (001) surfaces. The results presented above show that for every surface, except InSb(001), it is only the top one to two atomic layers that are affected by I_2 adsorption and annealing. This means that any sputter damage present in the initial clean surface that is deeper than 1–2 ML may not be removed by a I_2 dose-anneal cycle. These conclusions agree with LEED observations, where it was found that the quality of the patterns from

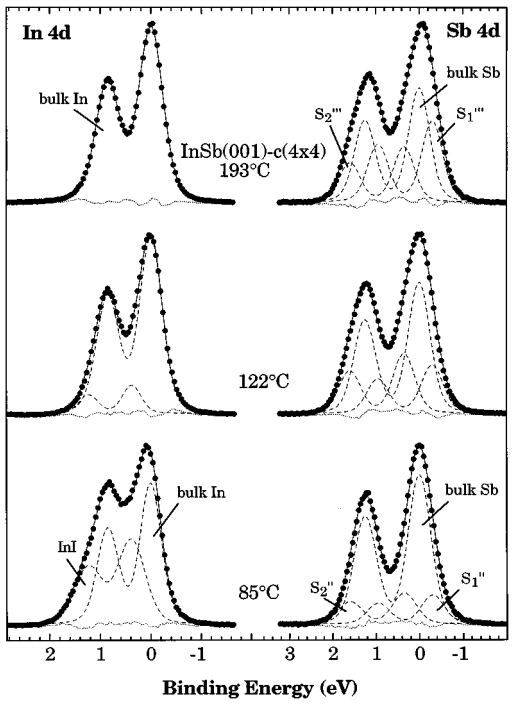

FIG. 15. High-resolution core-level spectra collected in normal emission from iodine-covered InSb(001) surfaces annealed to the temperatures shown, together with the results of a numerical fitting procedure. The legend for the symbols is the same as that in Fig. 4. The photon energy is 96 eV for both In and Sb levels.

the group-V-rich surfaces after iodine dosing and annealing were linked to the quality of the initial III-rich surface.

As seen in Fig. 13, iodine is removed at a lower temperature from InSb(001) than from InAs(001). If iodine leaves the surface as InI, then it is reasonable to assume that at least one In-Sb or In-As bond is broken in the process. The difference in removal temperatures could simply be related to the relative strengths of these bonds, since the In-Sb bond strength (1.57 eV for a diatomic bond) is smaller than that of In-As (2.08 eV).[46] This explanation is supported by annealing studies of iodine- and chlorine-covered InSb(001).[11] The removal temperature was found to be the same for both Cl and I, suggesting that the most important factor determining the adsorbate desorption temperature is the strength of the substrate III-V bond. Annealing studies of the I_2-saturated GaAs(001)-$c(2\times8)$ surface performed in the current study are also consistent with this idea. A temperature of 350 °C was required to remove all of the iodine from the GaAs surface, in agreement with the larger Ga-As bond strength (2.17 eV) as compared to In-As and In-Sb.

The lower removal temperature of InI from InSb(001) than from InAs(001), due to the smaller In-Sb substrate bond strength, has further implications regarding the presence or lack of RT etching for these substrates. The reason I_2 etches InSb(001)-c-(8×2) at RT, but not InAs(001)-$c(8\times2)$, is that there is a smaller barrier for the desorption of volatile gas-phase species, e.g., InI, from the InSb surface than from InAs. Similarly, the high removal temperature of iodine from GaAs(001), due to the strong Ga-As substrate bond, causes this surface to be saturated with I_2 at RT instead of etched. Note, however, that thermodynamics alone does not predict whether a substrate will or will not etch. Kinetic limitations imposed by the surface structure do play a role, since InSb(001)-$c(8\times2)$ is etched by I_2 at RT, while InSb(001)-$c(4\times4)$ is not.[11]

Iodine removal via annealing appears to occur much differently from the I_2-saturated group-V-element-terminated surfaces than from the -III-element-terminated surfaces. First, the LEED pattern observed after removing iodine from the (initially) As-rich GaAs(001)-$c(2\times8)$ surface also possessed a $c(2\times8)$ symmetry, but was noticeably weaker and less sharp. Second, the Ga/As core-level ratio was found to decrease by only 20% in this process, as compared to the factor of 2 observed for I_2-reacted InAs(001)-$c(8\times2)$ and InSb(001)-$c(8\times2)$. Since the same $c(2\times8)$ reconstruction is present before dosing and after iodine removal on GaAs(001), the simplest explanation is that iodine leaves this surface primarily as I_2. These results suggest that the interaction between GaAs(001)-$c(2\times8)$ and I_2 is almost ideally nondisruptive, producing minimal changes in the surface stoichiometry. Similar behavior for a -V-terminated surface was also reported by Jones, Singh, and McConville for InSb(001)-$c(4\times4)$.[11] They saw no changes in the In/Sb Auger ratio during dosing or heating of the $c(4\times4)$ surface.

Perhaps one of the more perplexing issues concerning the removal of iodine with annealing is the ease with which volatile group-III iodines form, as seen on In-terminated InAs and InSb, while volatile group-V iodines do not form on V-terminated surfaces. This difference in behavior can be summarized as a preference for breaking substrate bonds on iodine-covered group-III-terminated surfaces vs a preferential scission of the iodine-substrate bond for iodine-covered -V-terminated surfaces. The reason for the difference in behavior could be related to the fact that iodine-group-III-element bonds are, in general, stronger than iodine-group-V bonds.[46] Despite this preference, however, it is still thermodynamically favorable to form a group-V iodide rather than I_2, if only the volatile molecules are considered. The fact that As-As and Sb-Sb dimer bonds are three to four times stronger than Ga-Ga and In-In bonds,[46] however, may contribute towards a thermodynamically favorable reaction in which iodine leaves a -V-element-terminated surface as I_2, since additional group-V dimer bonds can then be created.

IV. SUMMARY

Molecular iodine generated by an electrochemical cell was reacted with InAs(001)-$c(8\times2)$, InSb(001)-$c(8\times2)$, and several reconstructions of GaAs(001). All InAs and GaAs surfaces show saturationlike behavior in the exposure range studied here. The saturated surfaces all possess very strong 1×1 LEED patterns, due to 1×1 ordering in both the overlayer and the near-surface region of the substrate. The removal of the clean surface reconstruction most likely occurs via the breakage of surface dimers and the formation of bonds between iodine and the surface atoms. This bonding primarily involves the outermost substrate atoms, although some bonding to the second-layer atoms may also occur. In contrast to InAs and GaAs, exposure of InSb(001)-$c(8\times2)$ to I_2 in excess of that needed to form the 1×1 structure results in etching of the substrate with preferential removal of In.

Annealing the iodine-covered In-rich InAs(001) and

InSb(001) surfaces results in the removal of the outermost layer of the substrate, producing a group-V-rich surface. Annealing the I_2-saturated As-rich GaAs(001)-$c(2\times8)$ surface, on the other hand, results in the desorption of iodine and the recovery of the $c(2\times8)$ LEED pattern. Thus, for all the (001) surfaces studied, dosing with I_2 followed by iodine removal via heating forms a group-V-rich surface without inducing large disruptions of the substrate order.

ACKNOWLEDGMENTS

The financial support of the Swedish Natural Science Research Council and NUTEK through the Nanometer Structure Consortium is gratefully acknowledged. We are obliged to B. P. Kowalski for the conductivity measurements characterizing the MBE system. J.A.Y. acknowledges the U.S. Army Research Office for partial support.

*Present address: Chemical Sciences Division, Lawrence Berkeley National Laboratory, Berkeley, CA 94720.

†Present address: Environmental Molecular Sciences Laboratory, Pacific Northwest National Laboratory, Richland, WA 99352.

[1] W. C. Simpson and J. A. Yarmoff, *Annual Reviews of Physical Chemistry* (Annual Reviews, Inc., Palo Alto, CA, 1996).

[2] C. Su, M. Xi, Z.-G. Dai, M. F. Vernon, and B. E. Bent, Surf. Sci. **282**, 357 (1993).

[3] J. C. Patrin, Y. Z. Li, M. Chander, and J. H. Weaver, Appl. Phys. Lett. **62**, 1277 (1993).

[4] K.-C. Wong and E. A. Ogryzlo, J. Vac. Sci. Technol. B **10**, 668 (1992).

[5] L. Hahn, K.-C. Wong, and E. A. Ogryzlo, J. Electrochem. Soc. **140**, 226 (1993).

[6] G. Margaritondo, J. E. Rowe, C. M. Bertoni, C. Calandra, and F. Manghi, Phys. Rev. B **20**, 1538 (1979).

[7] G. Margaritondo, J. E. Rowe, C. M. Bertoni, C. Calandra, and F. Manghi, Phys. Rev. B **23**, 509 (1981).

[8] J. C. Patrin and J. H. Weaver, Phys. Rev. B **48**, 17 913 (1993).

[9] P. R. Varekamp, M. C. Håkansson, D. K. Shuh, J. Kanski, L. Ilver, Z. Q. He, J. A. Yarmoff, and U. O. Karlsson, Vacuum **46**, 1231 (1995).

[10] A. P. Mowbray and R. G. Jones, Vacuum. **41**, 672 (1990).

[11] R. G. Jones, N. K. Singh, and C. F. McConville, Surf. Sci. **208**, L34 (1989).

[12] D. C. Flanders, L. D. Pressman, and G. Pinelli, J. Vac. Sci. Technol. B **8**, 1990 (1990).

[13] G. F. Doughty, S. Thoms, V. Law, and C. D. W. Wilkinson, Vacuum **36**, 803 (1986).

[14] L. M. Bharadwaj, P. Bonhomme, J. Faure, B. Balossier, and R. P. Bajpai, J. Vac. Sci. Technol. B **9**, 1440 (1991).

[15] U. K. Chakrabarti, S. J. Pearton, A. Katz, W. S. Hobson, and C. R. Abernathy, J. Vac. Sci. Technol. B **10**, 2378 (1992).

[16] U. K. Chakrabarti, F. Ren, S. J. Pearton, and C. R. Abernathy, J. Vac. Sci. Technol. A **12**, 1129 (1994).

[17] K. Jacobi, G. Steinert, and W. Ranke, Surf. Sci. **57**, 571 (1976).

[18] D. Troost, L. Koenders, and W. Mönch, Appl. Surf. Sci. **65/66**, 619 (1993).

[19] D. J. D. Sullivan, H. C. Flaum, and A. C. Kummel, J. Chem. Phys. **101**, 1582 (1994).

[20] D. K. Shuh, C. W. Lo, J. A. Yarmoff, A. Santoni, L. J. Terminello, and F. R. McFeely, Surf. Sci. **303**, 89 (1994).

[21] P. R. Varekamp, W. C. Simpson, D. K. Shuh, T. D. Durbin, V. Chakarian, and J. A. Yarmoff, Phys. Rev. B **50**, 14 267 (1994).

[22] M. O. Schweitzer, F. M. Leibsle, T. S. Jones, C. F. Mcconville, and N. V. Richardson, Surf. Sci. **280**, 63 (1993).

[23] C. F. McConville, T. S. Jones, F. M. Leibsle, and N. V. Richardson, Surf. Sci. **303**, L373 (1994).

[24] P. John, T. Miller, and T.-C. Chiang, Phys. Rev. B **39**, 1730 (1989).

[25] C. F. McConville, T. S. Jones, F. M. Leibsle, S. M. Driver, T. C. Q. Noakes, M. O. Schweitzer, and N. V. Richardson, Phys. Rev. B **50**, 14 965 (1994).

[26] D. K. Biegelsen, R. D. Bringans, J. E. Northrup, and L.-E. Swartz, Phys. Rev. B **41**, 5701 (1990).

[27] M. D. Pashley, K. W. Haberern, W. Friday, J. M. Woodall, and P. D. Kirchner, Phys. Rev. Lett. **60**, 2176 (1988).

[28] X. Hou, G. Dong, X. Ding, and X. Wang, J. Phys. C **20**, L121 (1987).

[29] P. R. Varekamp, M. C. Håkansson, J. Kanski, M. Björkqvist, M. Göthelid, B. J. Kowalski, Z. Q. He, D. K. Shuh, J. A. Yarmoff, and U. O. Karlsson, following paper, Phys. Rev. B **54**, 2114 (1996).

[30] N. D. Spencer, P. J. Goddard, P. W. Davies, M. Kitson, and R. M. Lambert, J. Vac. Sci. Technol. A **1**, 1554 (1983).

[31] U. O. Karlsson, J. N. Andersen, K. Hansen, and R. Nyholm, Nucl. Instrum. Methods A **282**, 553 (1989).

[32] A. P. Mowbray, R. G. Jones, and C. F. McConville, J. Chem. Soc. Faraday Trans. **87**, 3259 (1991).

[33] H. Gant and W. Mönch, Surf. Sci. **105**, 217 (1981).

[34] A. B. McLean, L. J. Terminello, and F. R. McFeely, Phys. Rev. B **40**, 11 778 (1989).

[35] D. Troost, L. Koenders, L.-Y. Fan, and W. Mönch, J. Vac. Sci. Technol. B **5**, 1119 (1987).

[36] F. Stepniak, D. Rioux, and J. H. Weaver, Phys. Rev. B **50**, 1929 (1994).

[37] K. Cierocki, D. Troost, L. Koenders, and W. Mönch, Surf. Sci. **264**, 23 (1992).

[38] C. B. M. Andersson, U. O. Karlsson, K. Ilver, J. Kanski, P. O. Nilsson, L. Ö. Olsson, and M. C. Håkansson, in *Proceedings of the 22nd International Conference on the Physics of Semiconductors, Vancouver, 1994*, edited by D. J. Lockwood (World Scientific, Singapore, 1995), p. 489.

[39] K. Smit, L. Koenders, and W. Mönch, J. Vac. Sci. Technol. B **7**, 888 (1989).

[40] R. Ludeke, T.-C. Chiang, and D. E. Eastman, Physica **117B&118B**, 819 (1983).

[41] J. F. van der Veen, P. K. Larsen, J. H. Neave, and B. A. Joyce, Solid State Commun. **49**, 659 (1984).

[42] J. N. Andersen and U. O. Karlsson, Phys. Rev. B **41**, 3844 (1990).

[43] P. K. Larsen, J. H. Neave, J. F. van der Veen, P. J. Dobson, and B. A. Joyce, Phys. Rev. B **27**, 4966 (1983).

[44] A. Mowbray and R. G. Jones, Appl. Surf. Sci. **48/49** 27 (1991).

[45] R. Tromp, G. W. Rubloff, P. Balk, F. K. L. Goues, and E. J. van Loenen, Phys. Rev. Lett. **55**, 2332 (1985).

[46] D. R. Lide and H. P. R. Rederikse, *CRC Handbook of Chemistry and Physics* (CRC, Boca Raton, 1995).

[47] D. E. Eastman and J. L. Freeouf, Phys. Rev. Lett. **34**, 1624 (1975).

[48] M. Taniguchi, S. Suga, M. Seki, S. Shin, K. L. I. Kobayashi, and H. Kanzaki, J. Phys. C **16**, L45 (1983).